Mixed Metal Cluster Chemistry. 10.[1] Isomer Distribution and Ligand Fluxionality at $CpWIr_3(\mu\text{-}CO)_3(CO)_{8-n}(PR_3)_n$ (n = 1, 2; R = Ph, Me)

Susan M. Waterman and Mark G. Humphrey*

Department of Chemistry, Australian National University, Canberra, A.C.T. 0200, Australia

Received April 21, 1999

The impact upon ligand coordination geometry and carbonyl fluxionality of heterometal incorporation into the prototypical tetrahedral cluster $Ir_4(CO)_{12}$ has been assessed. The isostructural $CpWIr_3(CO)_{11}$ (**1**) is related to $Ir_4(CO)_{12}$ by conceptual replacement of a late transition metal-containing $Ir(CO)_3$ vertex by a mid transition metal $CpW(CO)_2$ unit. This "very mixed" metal cluster has been derivatized by phosphines, the ligand fluxionality of the resultant clusters has been examined, and both the coordination geometry and CO mobility of the tungsten−iridium clusters have been contrasted with those of derivatives of the "parent" homometallic cluster. The tetrahedral clusters $CpWIr_3(\mu\text{-}CO)_3(CO)_{8-n}(L)_n$ [L = PPh_3, n = 1 (**2**), 2 (**3**); L = PMe_3, n = 1 (**4**), 2 (**5**)] are shown to exist as mixtures of interconverting isomers in solution. The structures of the isomers have been assigned using a combination of variable-temperature ^{31}P and ^{13}C NMR, COSY spectra and X-ray structural studies. All phosphine-containing clusters contain a carbonyl-bridged basal plane and an apical metal; ligands can be approximately coplanar (radial) to the basal plane or below the plane (axial). The configurations of **2a** and **4a** (axial phosphine, apical Cp, Ir_3 basal plane) and **2b** and **4b** (radial phosphine, radial or axial Cp, WIr_2 basal plane) are consistent with structural determinations of **4a** and **2b**; a third configuration (**2c**; axial phosphine, radial or axial Cp, WIr_2 basal plane) is observed only with the larger phosphine. The configurations of **3b** and **5b** (radial phosphine, axial phosphine, radial or axial Cp, WIr_2 basal plane) are consistent with a structural determination of **3b**, while a further configuration (**3a** and **5a**; diradial phosphines, radial Cp, WIr_2 basal plane) possesses a triradial coordination geometry. The configurations of **2a**, **3a**, **4a,** and **5a** are without precedent in monodentate ligand-substituted derivatives of the parent tetrairidium system. In contrast to reports with rhodium−iridium clusters, we find that the presence of the more electropositive tungsten does not polarize the electron distribution toward the iridiums and thereby favor an Ir_3 basal plane; rather, the WIr_2-bridged form is predominant across the isomers in the tungsten−iridium system. Suggested mechanisms of carbonyl fluxionality in the abundant isomers of **2**−**5**, assigned using ^{13}C exchange spectroscopy (EXSY) spectra, are proposed. Clusters **2a** and **4a**, with mutually trans phosphine and Cp, exchange carbonyls via a merry-go-round at Ir_3 and WIr_2 faces. Clusters **3a** and **5a** exchange all carbonyls by way of two processes: scrambling about the Ir_3 face to afford an intermediate with the carbonyl distribution of the D_{2d} form implicated in carbonyl mobility at $Ir_4(CO)_{12}$, and scrambling about a WIr_2 face by way of an all-terminal intermediate in which the putative merry-go-round process is blocked by phosphines and Cp.

Introduction

Ligand fluxionality on metal clusters has been the subject of many studies, with the majority of reports focusing on carbonyl migration on homometallic tri- and tetranuclear clusters.[2−11] The tetrahedral tetrairidium cluster core is robust, and facile routes into specifically substituted derivatives have been developed; not surprisingly, then, ligand-substituted derivatives of $Ir_4(CO)_{12}$ form one of the most extensively investigated systems.[12−32] Carbonyl scrambling on $Ir_4(CO)_{11}(L)$ derivatives is well-defined and proceeds by way of a Cotton

* Corresponding author. Ph: (+61) 2 6249 2927. Fax: (+61) 2 6249 0760. E-mail: Mark.Humphrey@anu.edu.au.

(1) Part 9: Waterman, S. M.; Humphrey, M. G.; Hockless, D. C. R. *J. Organomet. Chem.* **1998**, *565*, 81.
(2) Farrugia, L. J. *J. Chem. Soc., Dalton Trans.* **1997**, 1783.
(3) Roulet, R. *Chimia* **1996**, *50*, 629.
(4) Johnson, B. F. G.; Roberts, Y. V.; Parisini, E.; Benfield, R. E. *J. Organomet. Chem.* **1994**, *478*, 21.
(5) Orrell, K.; Sik, V. *Annu. Rep. NMR Spectrosc.* **1993**, *27*, 103.
(6) Orrell, K.; Sik, V. *Annu. Rep. NMR Spectrosc.* **1987**, *19*, 79.
(7) Mann, B. E. *Annu. Rep. NMR Spectrosc.* **1982**, *12*, 263.
(8) Band, E.; Muetterties, E. L. *Chem. Rev.* **1978**, *78*, 639.
(9) Johnson, B. F. G.; Benfield, R. E. *J. Chem. Soc., Dalton Trans.* **1978**, 1554.
(10) Shriver, D. F.; Kaesz, H. D.; Adams, R. D. *The Chemistry of Metal Cluster Complexes*; VCH.: New York, 1990.
(11) *Transition Metal Clusters*; Johnson, B. F. G., Ed.; Wiley: Cambridge, 1980.
(12) Laurenczy, G.; Bondietti, G.; Ros, R.; Roulet, R. *Inorg. Chim. Acta* **1996**, *247*, 65.
(13) Roberts, Y. V.; Johnson, B. F. G.; Benfield, R. E. *Inorg. Chim. Acta* **1995**, *229*, 221.

10.1021/om9902885 CCC: $18.00
Publication on Web 07/10/1999

Scheme 1: Merry-Go-Round Process in $Ir_4(\mu\text{-}CO)_3(CO)_8(L)$

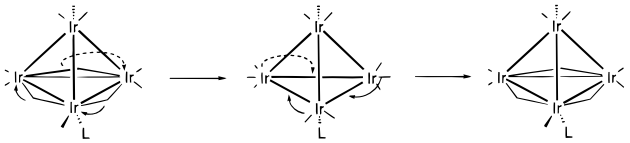

Scheme 2: Change of Basal Face Process in $Ir_4(\mu\text{-}CO)_3(CO)_8(L)$

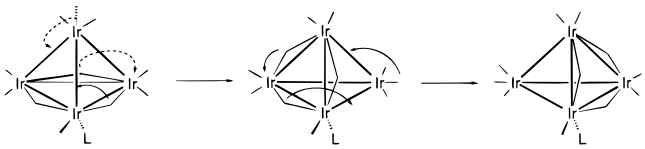

Scheme 3: Change of Basal Face Process in $Ir_4(\mu\text{-}CO)_3(CO)_7(cod)$ (Unbridged Intermediate)

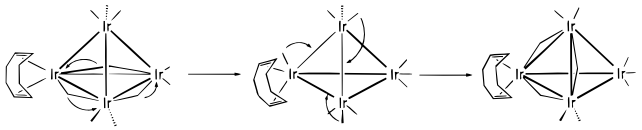

merry-go-round process (Scheme 1) or a mechanism with face-bridged intermediates (Scheme 2). Carbonyl fluxionality on $Ir_4(CO)_{10}(L)_2$ derivatives is a function of the carbonyl ligand distribution, specifically, the nature of the edge-bridging carbonyls. For $Ir_4(CO)_{10}(\eta^4\text{-cod})$ (cod = 1,5-cyclooctadiene) with a symmetric edge-bridged structure, carbonyl scrambling proceeds to give an unbridged intermediate, followed by re-formation of bridges about a different face (Scheme 3).[26] For clusters with asymmetric bridges, carbonyl scrambling occurs via a synchronous face change, as the short Ir−CO bridging bond is too strong to permit access to an unbridged intermediate (Scheme 4).

Scheme 4: Change of Basal Face Process in $Ir_4(\mu\text{-}CO)_3(CO)_7(diars)$ (Synchronous Face Change)

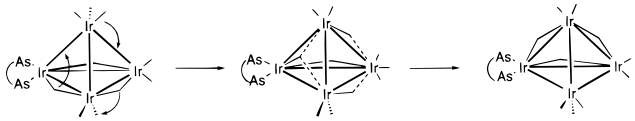

Carbonyl migration on heterometallic clusters has been the subject of significantly fewer studies than carbonyl mobility on homometallic clusters, although useful advantages accrue in the mixed metal system. Introduction of a heterometal lowers the molecular symmetry and may provide a label to facilitate assignment and to monitor carbonyl scrambling (particularly with NMR-active nuclei). As metals have differing propensities to stabilize the putative edge-bridged, face-capped, or all-terminal intermediates, heterometallic clusters should exhibit different activation energies for the various mechanisms of carbonyl migration, so that ligand mobility at specific ligated derivatives becomes accessible on the NMR time frame, or thermal discrimination of scrambling at specific faces or metals becomes possible. The fluxionality studies of $Ir_4(CO)_{12}$ summarized above have consequently been extended to $Ir_3Rh(CO)_{12}$ and $Ir_2Rh_2(CO)_{12}$,[33−36] with differences to the parent cluster ascribed to the differing electropositivities of the metals. The incorporation of a significantly more electropositive metal should accentuate such differences, but fluxionality studies of mixed metal clusters incorporating iridium and an early transition metal have not thus far been promulgated. The tetrahedral mixed metal cluster $CpWIr_3(CO)_{11}$ (**1**), conceptually derived from $Ir_4(CO)_{12}$ by replacement of an $Ir(CO)_3$ vertex with a $CpW(CO)_2$ unit, contains the electropositive tungsten; studies of ligand fluxionality at **1** and its derivatives are therefore of significant interest. We have recently reported the synthesis and characterization of the ligand-substituted derivatives $CpWIr_3(\mu\text{-}CO)_3(CO)_{8-n}(L)_n$ [L = PPh_3, n = 1 (**2**), 2 (**3**); L = PMe_3, n = 1 (**4**), 2 (**5**)],[37] benchmarking the reaction rates in a qualitative sense against those of the "parent" cluster $Ir_4(CO)_{12}$; for the "very mixed" metal system, reactions proceed in a stepwise fashion in minutes at room temperature, in contrast to the homometallic cluster, where reaction requires forcing conditions or use of activated precursors. The clusters exist as mixtures of interconverting isomers in solution. In our earlier report, the configurations of these isomers could not be conclusively identified, but the isomers were tentatively assigned coordination geometries based on limited X-ray structural studies and ^{31}P NMR spectroscopic data. The present report includes conclusive identification of the geometries of the major isomers of clusters **2**−**5**, informed speculation as to the mechanisms of fluxionality at these "very mixed" metal clusters, and a comparison of isomer structure and fluxionality with that observed

(14) Strawczynski, A.; Hall, C.; Bondietti, G.; Ros, R.; Roulet, R. *Helv. Chim. Acta* **1994**, *77*, 754.
(15) Strawczynski, A.; Suardi, G.; Ros, R.; Roulet, R. *Helv. Chim. Acta* **1993**, *76*, 2210.
(16) Besançon, K.; Laurenczy, G.; Lumini, T.; Roulet, R. *Helv. Chim. Acta* **1993**, *76*, 2926.
(17) Bondietti, G.; Ros, R.; Roulet, R.; Musso, F.; Gervasio, G. *Inorg. Chim. Acta* **1993**, *213*, 301.
(18) Johnson, B. F. G.; Roberts, Y. V. *Inorg. Chim. Acta* **1993**, *205*, 175.
(19) Davis, M. J.; Roulet, R. *Inorg. Chim. Acta* **1992**, *197*, 15.
(20) Mann, B. E.; Vargas, M. D.; Khadar, R. *J. Chem. Soc., Dalton Trans.* **1992**, 1725.
(21) Orlandi, A.; Frey, U.; Suardi, G.; Merbach, A. E.; Roulet, R. *Inorg. Chem.* **1992**, *31*, 1304.
(22) Strawczynski, A.; Ros, R.; Roulet, R.; Braga, D.; Gradella, C.; Grepioni, F. *Inorg. Chim. Acta* **1990**, *170*, 17.
(23) Suardi, G.; Strawczynski, A.; Ros, R.; Roulet, R. *Helv. Chim. Acta* **1990**, *73*, 154.
(24) Mann, B. E.; Pickup, B. T.; Smith, A. K. *J. Chem. Soc., Dalton Trans.* **1989**, 889.
(25) Strawczynski, A.; Ros, R.; Roulet, R. *Helv. Chim. Acta* **1988**, *71*, 867.
(26) Strawczynski, A.; Ros, R.; Roulet, R. *Helv. Chim. Acta* **1988**, *71*, 1885.
(27) Ros, R.; Scrivanti, A.; Albano, V. G.; Braga, D. *J. Chem. Soc., Dalton Trans.* **1986**, 2411.
(28) Braga, D.; Ros, R.; Roulet, R. *J. Organomet. Chem.* **1985**, *286*, C8.
(29) Mann, B. E.; Spencer, C. M.; Smith, A. K. *J. Organomet. Chem.* **1983**, *244*, C17.
(30) Stuntz, G. F.; Shapley, J. R. *J. Organomet. Chem.* **1981**, *213*, 389.
(31) Stuntz, G. F.; Shapley, J. R. *J. Am. Chem. Soc.* **1977**, *99*, 607.
(32) Cattermole, P. E.; Orrell, K. G.; Osborne, A. G. *J. Chem. Soc., Dalton Trans.* **1974**, 328.
(33) Bondietti, G.; Laurenczy, G.; Ros, R.; Roulet, R. *Helv. Chim. Acta* **1994**, *77*, 1869.
(34) Bondietti, G.; Ros, R.; Roulet, R.; Grepioni, F.; Braga, D. *J. Organomet. Chem.* **1994**, *464*, C45.
(35) Laurenczy, G.; Bondietti, G.; Merbach, A. E.; Moullet, B.; Roulet, R. *Helv. Chim. Acta* **1994**, *77*, 547.
(36) Bondietti, G.; Suardi, G.; Ros, R.; Roulet, R.; Grepioni, F.; Braga, D. *Helv. Chim. Acta* **1993**, *76*, 2913.
(37) Waterman, S. M.; Humphrey, M. G.; Tolhurst, V.-A.; Skelton, B. W.; White, A. H. *Organometallics* **1996**, *15*, 934.

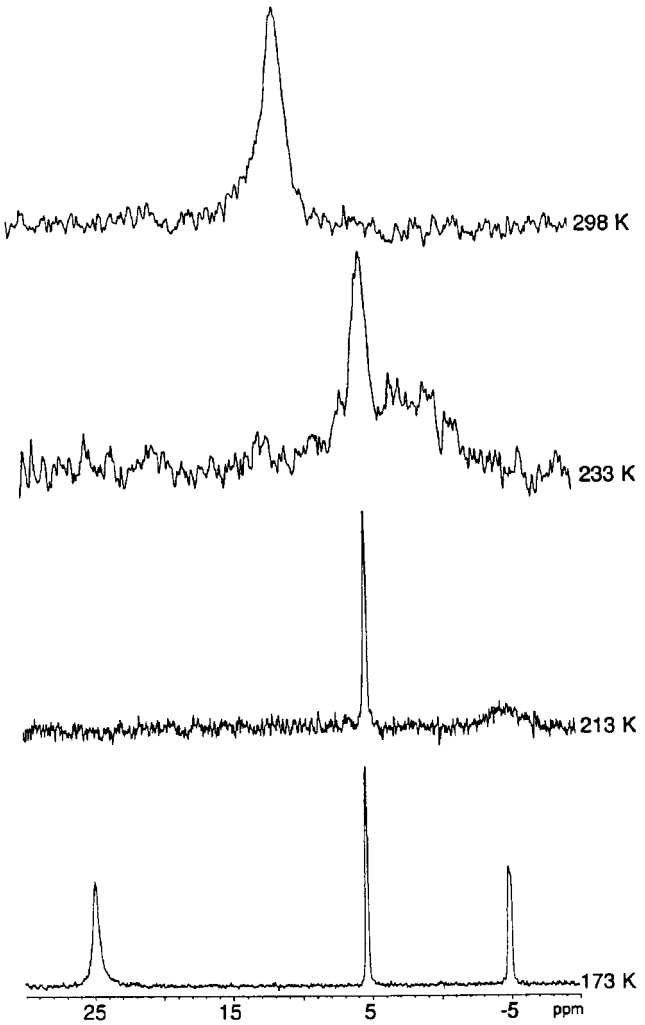

Figure 1. Variable-temperature ^{31}P NMR spectroscopic study of $CpWIr_3(\mu\text{-}CO)_3(CO)_7(PPh_3)$ (**2**) in CD_2Cl_2.

in the "parent" tetrairidium system, to benchmark the significance of the heterometallic environment for these fundamentally important properties.

Experimental Section

Syntheses. $CpWIr_3(CO)_{11}$ (**1**)[38] and $CpWIr_3(\mu\text{-}CO)_3(CO)_{8-n}(PR_3)_n$ (n = 1, 2, R = Me, Ph) (**2**−**5**)[37,39] were synthesized according to literature procedures. ^{13}CO-enriched samples were prepared from ^{13}CO-enriched (65%) **1**, itself obtained by stirring a solution of the cluster in CH_2Cl_2 under 1.2 atm ^{13}CO at 60 °C for 48 h.

NMR Studies. NMR spectra were recorded on a Varian VXR300S spectrometer (^{13}C at 75 MHz and ^{31}P at 121 MHz) in either CD_2Cl_2 (Cambridge Isotope Laboratories), $4CS_2$:$1CD_2Cl_2$ (CS_2, Univer; CD_2Cl_2, Cambridge Isotope Laboratories), or toluene-d_8 (Cambridge Isotope Laboratories). References for the ^{13}C NMR spectra are the residual solvent peak resonances, with their chemical shifts relative to $SiMe_4$ = 0.0 ppm. ^{13}C NMR spectra are proton decoupled. Resonances are reported in the following form: ppm (assignment; multiplicity; relative intensity), with the specific assigned sites shown in Figure 3. The ^{31}P NMR spectra are reported relative to external 85% H_3PO_4 at 0.0 ppm. The $^{13}C\{^1H\}$ EXSY experiments were carried out using the standard NOESY pulse sequence with

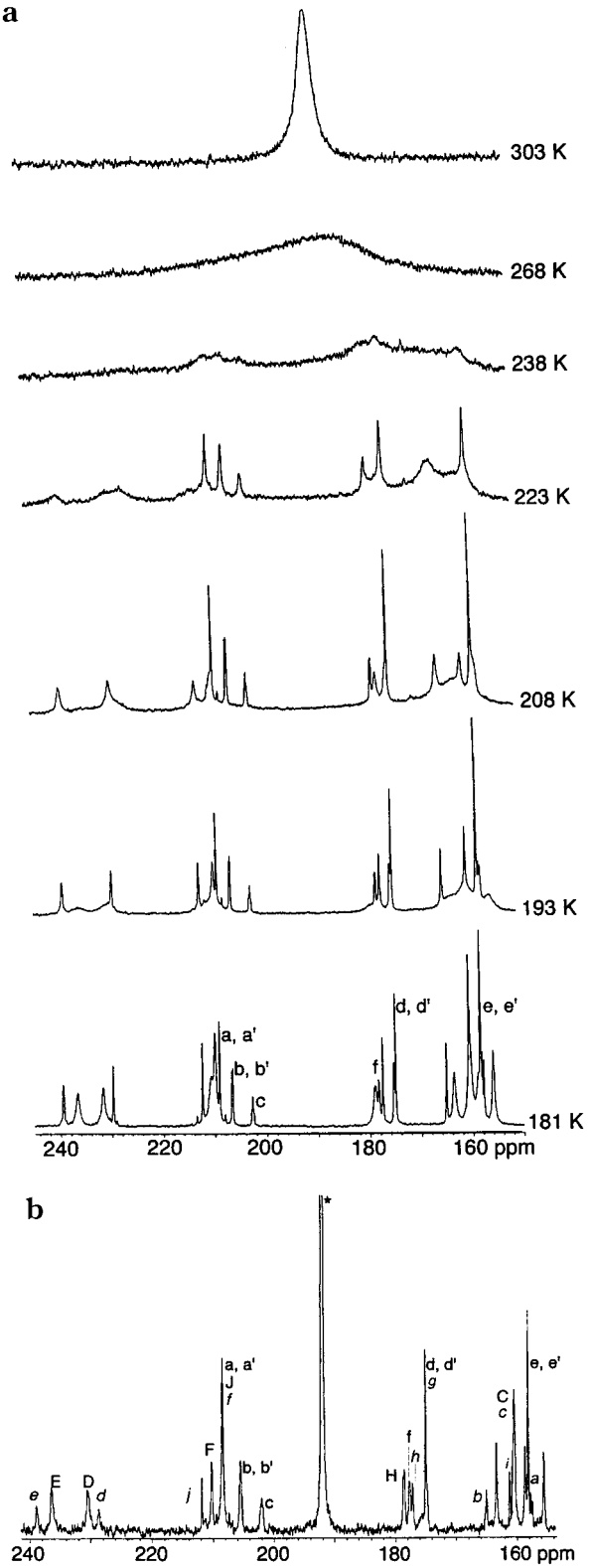

Figure 2. (a) Variable-temperature ^{13}C NMR spectroscopic study of $CpWIr_3(\mu\text{-}CO)_3(CO)_7(PPh_3)$ (**2**) in CD_2Cl_2. (b) ^{13}C NMR spectrum of $CpWIr_3(\mu\text{-}CO)_3(CO)_7(PPh_3)$ (**2**) in CS_2/CD_2Cl_2 at 163 K (★ ≡ CS_2).

the mixing time set to 0.05 s. The $^{13}C-^{13}C$ COSY experiments were carried out using the standard homonuclear chemical shift correlation pulse sequence on the Varian VXR300S spectrometer. The integrated ^{13}C NMR spectra were recorded with a recycle delay of 3−5 times the longest T_1 of the carbonyl ligands. 2D NMR spectra were recorded utilizing a recycle delay of 1−3 times the longest T_1 of the carbonyl ligands. T_1

(38) Shapley, J. R.; Hardwick, S. J.; Foose, D. S.; Stucky, G. D. *J. Am. Chem. Soc.* **1981**, *103*, 7383.
(39) Lee, J.; Humphrey, M. G.; Hockless, D. C. R.; Skelton, B. W.; White, A. H. *Organometallics* **1993**, *12*, 3468.

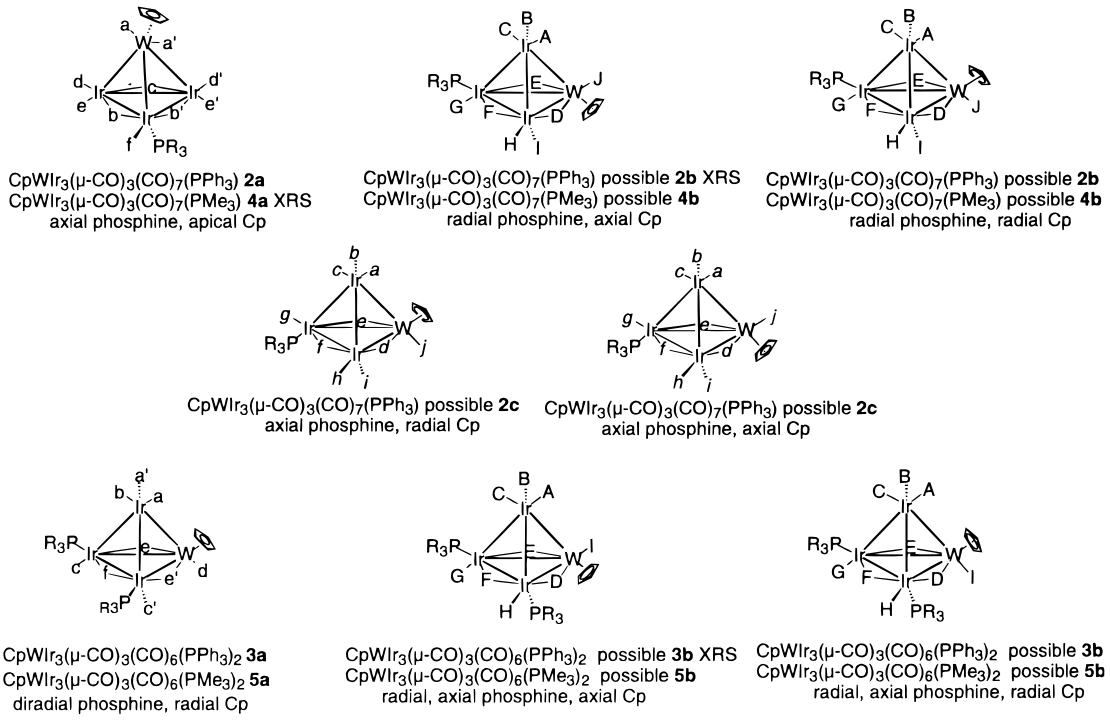

Figure 3. Isomers of $CpWIr_3(\mu\text{-}CO)_3(CO)_{8-n}(L)_n$ (L = PPh_3, PMe_3; n = 1, 2); r = radial, ax = axial, ap = apical. XRS ≡ X-ray crystallographic study exists.

measurements were carried out employing the standard inversion−recovery procedure.

Spectroscopic Data. (a) $CpWIr_3(\mu\text{-}CO)_3(CO)_7(PPh_3)$ (2). ^{13}C NMR (CD_2Cl_2, 181 K) **2a**: 208.3 (a, a′; s, 85%, d, 15%, J_{WC} = 154 Hz; 1.0), 205.4 (b, b′; s; 1.0), 201.9 (c; s; 0.5), 178.0 (f; s; 0.5), 174.9 (d, d′; s; 1.0), 158.0 (e, e′; s; 1.0) ppm. **2b**: 238.9 (E; br s; 0.3), 230.9 (D; br s; 0.3), 209.9 (F; br s; 0.3), 209.2 (J; s; 0.3), 178.6 (H; br s; 0.3), 160.3 (C; s; 0.3), other signals not assigned. **2c**: 238.6 (*e*; s, 85%, d, 15%, J_{WC} = 71 Hz; 0.2), 228.9 (*d*; s, 85%, d, 15%, J_{WC} = 72 Hz; 0.2), 211.6 (*j*; s, 85%, d, 15%, J_{WC} = 171 Hz; 0.2), 209.2 (*f*; s, 0.2), 177.2 (*h*; s, 0.2), 174.9 (*g*; s, 0.2), 162.5 (*b*; s, 0.2), 160.3 (*c*; s; 0.2), 157.9 (*a*; d J_{PC} = 15 Hz; 0.2), *i* not assigned. ^{13}C NMR (CS_2/CD_2Cl_2, 163 K) **2a**: 208.4 (a, a′; s; 1.0), 205.7 (b, b′; s; 1.0), 202.0 (c; s; 0.5), 177.7 (f; s; 0.5), 174.9 (d, d′; s; 1.0), 157.9 (e, e′; s; 1.0) ppm. **2b**: 235.6 (E; s; 0.3), 230.5 (D; s; 0.3), 210.2 (F; s; 0.3), 208.4 (J; s; 0.3), 178.5 (H; br s, 0.3), 160.3 (C; s; 0.3), other signals not assigned. **2c**: 238.9 (*e*; s; 0.2), 228.6 (*d*; s; 0.2), 211.8 (*j*; s; 0.2), 208.4 (*f*; s, 0.2), 177.1 (*h*; s; 0.2), 174.9 (*g*; s; 0.2), 164.9 (*b*; s; 0.2), 160.3 (*i*; s; 0.2), 160.0 (*c*; s; 0.2), 157.7 (*a*; d J_{PC} = 15 Hz; 0.2). ^{31}P NMR (CD_2Cl_2, 173 K): 24.9 (0.3P, **2b**), 5.3 (0.5P, **2a**), −4.9 (0.2P, **2c**) ppm.

(b) $CpWIr_3(\mu\text{-}CO)_3(CO)_6(PPh_3)_2$ (3). ^{13}C NMR (CD_2Cl_2, 191 K) **3a**: 241.0 (e, e′; s, 85%, d, 15%, J_{WC} = 73 Hz; 1.8), 217.0 (f; s; 0.9), 212.8 (d; s, 85%, d, 15%, J_{WC} = 172 Hz; 0.9), 167.5 (b; s; 0.9), 162.2 (a, a′; s; 1.8), 157.3 (c, c′; s; 1.8) ppm. **3b**: 243.1 (D or E; s; 0.1), 237.4 (E or D; s; 0.1), 228.0 (F; s; 0.1), 214.1 (I; s; 0.1), 177.6 (H; dd $^2J_{CP}$ = 22 Hz, $^3J_{CP}$ = 10 Hz; 0.1), 164.7 (C or B; s; 0.1), 161.5 (G; d $^2J_{CP}$ = 22 Hz; 0.1), 161.5 (A; s; 0.1), 156.2 (B or C; s; 0.1) ppm. ^{31}P NMR (CD_2Cl_2, 191 K): 27.4 (1.8P, **3a**), 26.1 (0.1P, **3b**), −7.0 (0.1P, **3b**) ppm.

(c) $CpWIr_3(\mu\text{-}CO)_3(CO)_7(PMe_3)$ (4). ^{13}C NMR ($4CS_2$:$1CD_2Cl_2$, 163 K) **4a**: 209.5 (a, a′; s, 85%, d, 15%, J_{WC} = 152 Hz; 0.76), 206.6 (b, b′; s; 0.76), 202.2 (c′; s; 0.38), 177.7 (f; s; 0.38), 174.9 (d, d′; s; 0.76), 158.0 (e, e′; s; 0.76) ppm. **4b**: 240.6 (E; s;, 85%, d, 15%, J_{WC} = 71 Hz; 0.62), 232.2 (D; s, 85%, d, 15%, J_{WC} = 71 Hz; 0.62), 211.6 (F; s; 0.62), 210.8 (J; s, 85%, d, 15%, J_{WC} = 152 Hz; 0.62), 179.4 (H; s; 0.62), other signals not assigned. ^{31}P NMR (CD_2Cl_2, 173 K): −31.8 (0.38P, **4a**), −25.0 (0.62P, **4b**) ppm.

(d) $CpWIr_3(\mu\text{-}CO)_3(CO)_6(PMe_3)_2$ (5). ^{13}C NMR (CD_2Cl_2, 193 K) **5a**: 247.4 (e, e′; s, 85%, d, 15%, J_{WC} = 73 Hz; 1.82), 225.9 (f; s; 0.91), 214.8 (d; s, 85%, d, 15%, J_{WC} = 178 Hz; 0.91), 167.5 (b; s; 0.91), 164.0 (a, a′; s; 1.82), 162.2 (c, c′; s; 1.82) ppm. **5b**: 249.0 (D or E; s; 0.09), 244.9 (E or D; s; 0.09), 225.8 (F; s; 0.09), 216.0 (I; s; 0.09), 180.8 (H; dd $^2J_{CP}$ = 22 Hz, $^3J_{CP}$ = 10 Hz; 0.09), 166.7 (C or B; s; 0.09), 165.4 (A; s; 0.09), 163.2 (G, d $^2J_{CP}$ = 22 Hz; 0.09), 159.4 (B or C; s; 0.09). ^{31}P NMR (CD_2Cl_2, 193 K): −21.8 (1.82P, **5a**), −23.6 (0.09P, **5b**), − 41.0 (0.09P, **5b**) ppm.

Results and Discussion

NMR Studies of $CpWIr_3(\mu\text{-}CO)_3(CO)_7(PPh_3)$ (2). The room-temperature ^{31}P NMR spectrum of **2** in CD_2Cl_2 contains a broad singlet at 10.1 ppm. On cooling to 173 K, three signals are resolved at 24.9, 5.3, and −4.9 ppm in the ratio 3:5:2 (Figure 1). Shapley has previously noted that the ^{31}P NMR chemical shift sequence radial > axial is observed with tetrairidium clusters,[31] and its application to **2** leads us to assign the resonance at 24.9 ppm to an isomer with phosphine occupying a radial site, and the resonances at 5.3 and −4.9 ppm to isomers with phosphines in axial sites. The room-temperature ^{13}C NMR spectrum of **2** consists of a broad singlet at 192.8 ppm. On cooling to 181 K, the spectrum splits into signals corresponding to three isomers in the approximate ratio 3:5:2 (Figure 2), consistent with the ^{31}P NMR spectra. Due to solubility, relative abundance, and other experimental problems, we have thus far completed isomer assignment and fluxionality studies for only one of the three isomers (**2a**: see below). The structures of the three isomers of **2** can be assigned from the extant ^{31}P NMR data and ^{13}C NMR data (Figure 3). We have extended the NMR chemical shift positional sequence established with tetrairidium clusters (bridging > radial > axial ≈ apical [27]) to the mixed-metal regime, affording the chemical shift sequence W−W

bridging CO > W−Ir bridging CO > Ir−Ir bridging CO ≈ W terminal CO > Ir radial CO > Ir axial CO ≈ Ir apical CO (a summary of data substantiating this sequence is available as Supporting Information); it is possible to distinguish Ir−Ir bridging carbonyls from W terminal carbonyls due to the 15% abundant ^{183}W-coupled satellites of the latter. With this information, it is then possible to assign the spectrum of **2a** and confirm its coordination geometry. At 181 K, resonances for isomer **2a** are observed at 208.3 (a, a′), 205.4 (b, b′), 201.9 (c), 177.6 (f), 174.9 (d, d′), and 158.0 (e, e′) ppm with the relative intensities 2:2:1:1:2:2, and the signal for the W-ligated a, a′ at 208.3 ppm showing the expected coupling to ^{183}W (J_{WC} = 154 Hz). We have noted elsewhere[40] that coupling constants for terminally coordinated carbonyls (J_{WC} 150−200 Hz) are significantly larger than those for bridging carbonyls (J_{WC} 75−100 Hz); the presence of two W-bound terminal carbonyl ligands, together with signals integrating to three carbonyl ligands in the Ir−Ir bridging carbonyl region, confirms that **2a** possesses a triiridium basal plane. The signals at 205.4 and 201.9 ppm are assigned to the Ir−Ir bridging carbonyls b, b′ and c, respectively. The signals at 177.6 and 174.9 ppm are assigned to the Ir-ligated radial carbonyls f and d, d′, respectively, with the remaining signal at 158.0 ppm being assigned to the Ir-coordinated axial carbonyls e, e′. The molecular symmetry evident from the ^{13}C NMR spectrum is consistent with configuration **2a** (Figure 3), for which a crystallographically characterized precedent exists (**4a**: see below). A ^{13}C−^{13}C correlation spectroscopy (COSY) experiment (Figure 4) reveals coupling between the Ir−Ir bridging carbonyls b, b′ and c, but long-range trans coupling between the carbonyls a, a′ and e, e′ was not observed. The crystallographically observed isomer of **2**[37] has a basal WIr_2 plane with Cp occupying an axial site and PPh_3 occupying a radial site (radial, axial isomer) and is possibly responsible for the most downfield signal in the ^{31}P NMR spectrum (see above). At 163 K, the ^{13}C NMR spectrum of **2** in CS_2/CD_2Cl_2 (Figure 2b) reveals resonances for configuration **2b,** which are cautiously assigned as 236.4 (E), 230.5 (D), 210.2 (F), 208.4 (J), 178.5 (H), and 160.3 (C) ppm, but discrimination between the remaining axial and apical carbonyl resonances is not possible. A Gaussian weighting function was used to identify the ^{183}W-coupled satellite signals for carbonyls E, D, and J. The signal at 210.2 is assigned to the Ir−Ir bridging carbonyl F due to its coupling with the W−Ir bridging carbonyls D and E, as shown in the COSY experiment (Figure 4). The bridging carbonyl resonances confirm that isomer **2b** possesses a WIr_2 basal plane. The signal at 178.5 is assigned to the Ir-ligated radial carbonyl H. There are two possible configurations consistent with the ^{31}P and ^{13}C NMR data (the cyclopentadienyl ligand may be radially or axially disposed), and it is not possible to discriminate between them on the basis of the spectral data. It is perhaps significant that one of the two possible configurations (depicted in Figure 3) has been identified in an X-ray structural study.[37] The remaining signal in the axial phosphine region of the ^{31}P NMR (−4.9 ppm) is assigned to a third isomer, **2c**, with an axial PPh_3. At 163 K in the ^{13}C NMR spectrum, resonances for configuration **2c** are observed at 238.9 (*e* or *d*), 228.6 (*d* or *e*), 211.8 (*j*), 208.4 (*f*), 177.1 (*h*), 174.9 (*g*), 164.9, 160.3, 160.0 (*b*, *i*, and *c*), and 157.7 (*a*) ppm, all of relative intensity 1. As before, a Gaussian weighting function was used to identify the ^{183}W satellites of carbonyls *e*, *d*, and *j*, with the former two assigned as W−Ir bridging CO's, and the last-mentioned assigned as a W-bound terminal CO. The signal at 208.4 is assigned to the Ir−Ir bridging carbonyl *f* from its coupling to the W−Ir bridging carbonyls *d* and *e*, as observed in the COSY spectrum (Figure 4). These data confirm the presence of a WIr_2 basal plane. The signals at 177.1 and 174.9 ppm are assigned to the Ir-ligated radial carbonyls *h* and *g*, by their respective lack or presence of cis P−C coupling. The signal at 157.7 ppm is assigned to the apical carbonyl *a* from its long-range trans coupling to PPh_3. As with **2b**, the remaining uncertainty with **2c** is the location of the basal cyclopentadienyl ligand. The sterically demanding cyclopentadienyl (cone angle: 136°) and triphenylphosphine (145°) ligands would disfavor diaxial ligation and render the alternative radial Cp, axial phosphine geometry more likely, but we are unable to confirm this with existing spectral data.

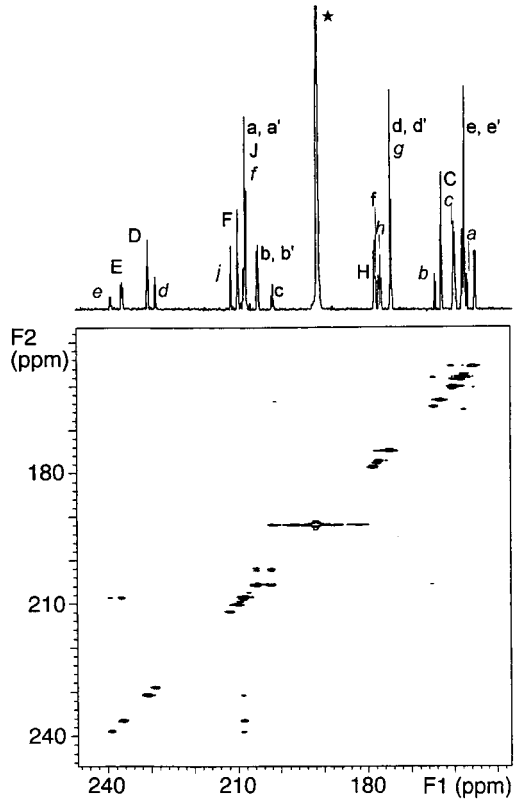

Figure 4. ^{13}C NMR COSY spectrum of $CpWIr_3(\mu\text{-}CO)_3(CO)_7(PPh_3)$ (**2**) in CS_2/CD_2Cl_2 at 173 K (★ ≡ CS_2).

Ligand fluxionality commences upon warming the mixture of isomers of **2**. A ^{13}C{^{1}H} EXSY study at 218 K is shown in Figure 5. EXSY experiments use a NOESY sequence which allows for a "mixing time" during which the observed nuclei may migrate to another site. The EXSY spectrum for **2** was performed in toluene-d_8 rather than the CD_2Cl_2 in which the ^{31}P and ^{13}C NMR spectra were run, to change the ratio of isomers in favor of isomer **2a** and facilitate the detection

(40) Waterman, S. M.; Humphrey, M. G.; Lee, J.; Ball, G. E.; Hockless, D. C. R. *Organometallics* **1999**, *18*, 2440.

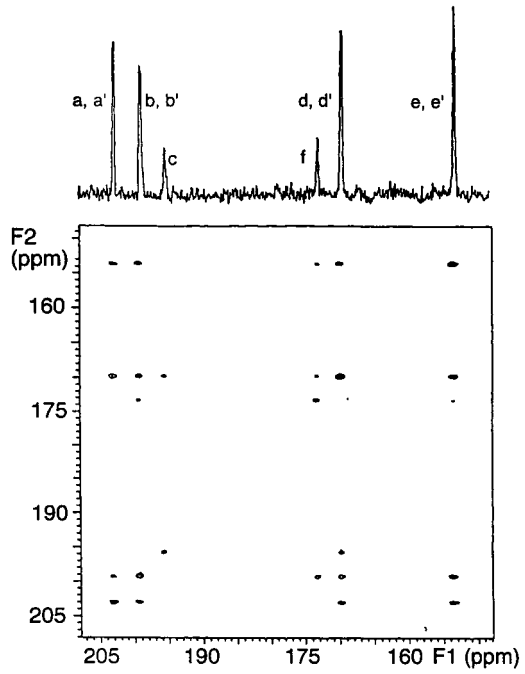

Figure 5. ^{13}C NMR EXSY spectrum of $CpWIr_3(\mu\text{-}CO)_3(CO)_7(PPh_3)$ (**2**) in toluene-d_8 at 218 K.

of cross-peaks. The contour plot for isomer **2a** (218 K) reveals site exchanges corresponding to a, a′ ↔ b, b′; a, a′ ↔ d, d′; a, a′ ↔ e, e′; b, b′ ↔ d, d′; b, b′ ↔ e, e′; b, b′ ↔ f; d, d′ ↔ e, e′; and c ↔ d, d′. This is consistent with the carbonyls exchanging via a concerted merry-go-round process, by way of an all-terminal intermediate (Scheme 5). All carbonyls are involved in the exchange process, either by re-formation of the Ir_3-bridged face or by formation of a WIr_2-bridged face. The only position blocked for merry-go-round exchange is that trans to the phosphine (occupied by the cyclopentadienyl ligand). The exchange process is thus analogous to that observed in $Ir_4(CO)_{11}(PMe_2Ph)$, where all carbonyls are fluxional with the exception of the unique carbonyl trans to the phosphine.[31] We were not able to utilize the integrated EXSY cross-peaks to afford rate data and confirm that the CO scrambling that affords the WIr_2-bridged intermediate has the same activation energy as re-formation of the Ir_3-bridged structure; however, a qualitative inspection reveals no evidence for Ir_3 bridge re-forming being a lower energy process than WIr_2 bridge formation (incorporation of the electropositive tungsten may polarize cluster electron density toward the Ir_3 face and thereby stabilize bridging carbonyls about this face).

NMR Studies of $CpWIr_3(\mu\text{-}CO)_3(CO)_6(PPh_3)_2$ (3). The room-temperature ^{13}C and ^{31}P NMR spectra of **3** in CD_2Cl_2 reveal broadened resonances, but at 191 K the fluxional processes have slowed sufficiently to reveal three signals in the ^{31}P NMR spectrum (ratio 16:1:1) and distinguish resonances corresponding to two isomers in the ^{13}C NMR spectrum (Figures 6 and 7). The ^{31}P NMR spectrum suggests the presence of a major isomer with two radially coordinated phosphines (**3a**) and a minor isomer with radial and axial coordinated phosphines (**3b**) (Figure 3). At 191 K, resonances for the more abundant isomer are observed in the ^{13}C NMR spectrum at 241.0 (e, e′), 217.0 (f), 212.8 (d), 167.5 (b), 162.2 (a, a′), and 157.3 (c, c′) ppm, with intensities 2:1:

Scheme 5: Merry-Go-Round Process in 2a and 4a

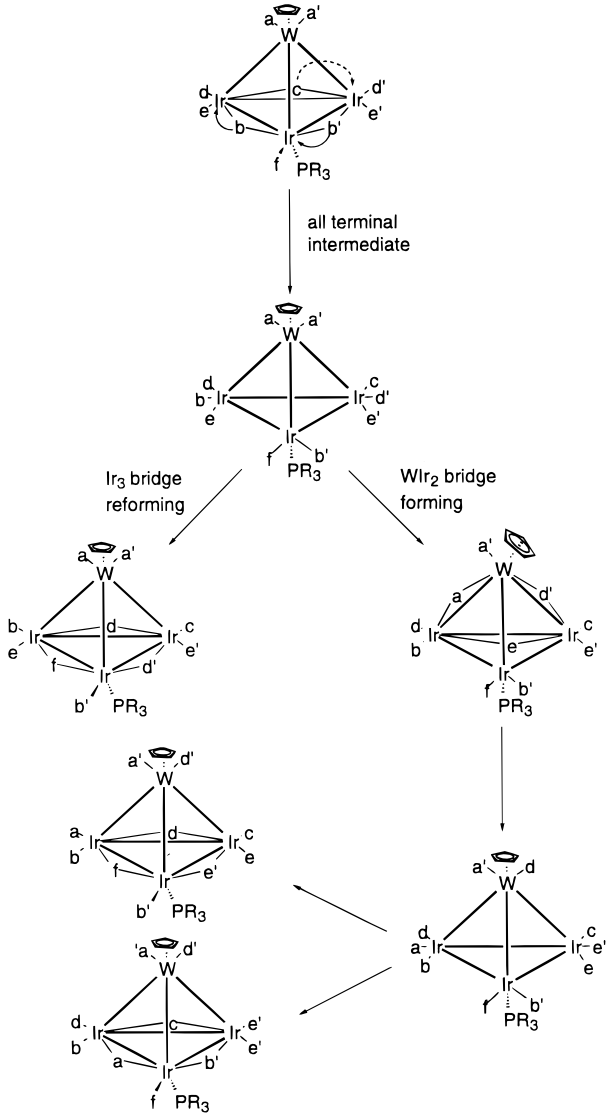

1:1:2:2. The signals at 241.0 and 212.8 ppm show satellite coupling to ^{183}W (J_{WC} = 73 and 172 Hz, respectively) and were therefore assigned as W−Ir bridging and W-ligated terminal carbonyls, respectively, which establishes the presence of a WIr_2 basal plane. The remaining uncertainty is the location of the cyclopentadienyl ligand, which can be radially or axially disposed. A $^{13}C-^{13}C$ correlation spectroscopy (COSY) experiment was used to establish its position (Figure 8); the presence of a long-range trans coupling between carbonyls b and d revealed that d is axially ligated and that the Cp ligand is radially coordinated. Isomer **3a** is therefore an example of a trisubstituted tetrahedral cluster with an unprecedented triradial geometry (Figure 3). The signal at 217.0 ppm is assigned to the Ir−Ir bridging carbonyl f, and the signal at 157.3 ppm to the iridium-coordinated axial carbonyls c, c′; carbonyls c, c′ are distinguished from carbonyls a, a′ by the presence of couplings in the $^{13}C-^{13}C$ COSY experiment [the signal at 157.3 ppm (c, c′) shows a cross-peak with the signal at 241.0 ppm (the adjacent bridging carbonyls e, e′) and a long-range trans coupling with the signal at 162.2 ppm (a, a′)] (Figure 8). The coupling between the axial carbonyls (e, e′) and the W−Ir bridging carbonyls (c, c′) is unusual, but the alternative [assigning the

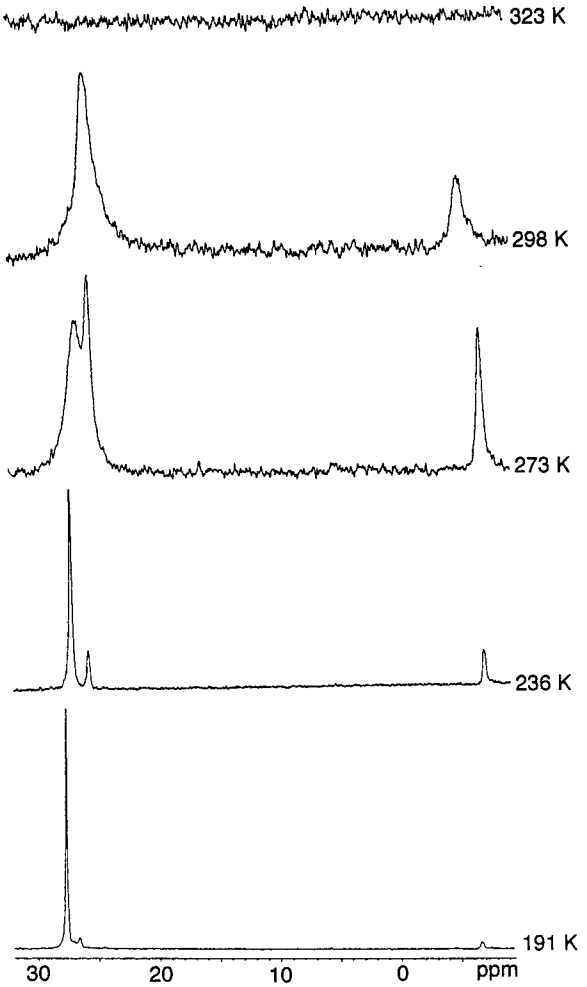

Figure 6. Variable-temperature ^{31}P NMR spectroscopic study of $CpWIr_3(\mu\text{-}CO)_3(CO)_6(PPh_3)_2$ (**3**) in CD_2Cl_2.

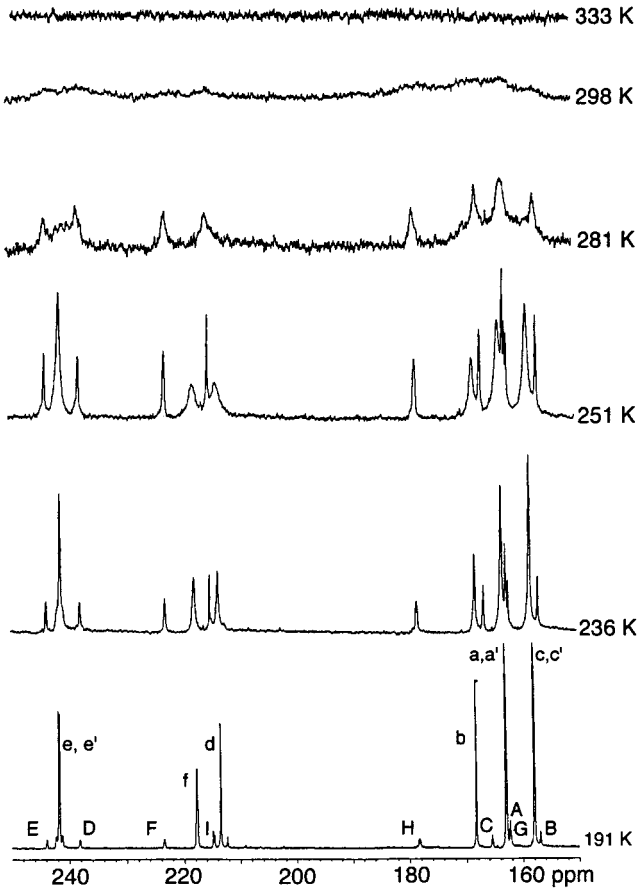

Figure 7. Variable-temperature ^{13}C NMR spectroscopic study of $CpWIr_3(\mu\text{-}CO)_3(CO)_6(PPh_3)_2$ (**3**) in CD_2Cl_2.

signals at 157.3 ppm (**3a**) and 162.2 ppm (in the analogous **5a**: see below) to the apical carbonyls (a, a′) and coupling between apical carbonyls and W−Ir bridging carbonyls in the basal plane] is much less likely. The signals at 167.5 and 162.2 ppm are assigned to the apical carbonyls b and a, a′, respectively. As mentioned above, the minor isomer (**3b**) possesses radially and axially ligated phosphines. Resonances for isomer **3b** are observed in the ^{13}C NMR spectrum at 243.1 (D or E), 237.4 (E or D), 228.0 (F), 214.1 (I), 177.6 (H), 164.7 (C or B), 161.5 (G), 161.5 (A), and 156.2 (B or C) ppm, all with intensity 1. The presence of signals integrating to two carbonyls in the W−Ir bridging CO region and four carbonyls in the axial/apical Ir ligated CO region is consistent only with a WIr_2 basal plane. Radially and axially disposed phosphines are suggested by the ^{31}P NMR data. The remaining uncertainty is therefore the position of the cyclopentadienyl ligand, which can be radially or axially ligated. The two possible configurations are shown in Figure 3. It is perhaps significant that one of these two configurations has been observed in a structural study.[37] The ^{13}C NMR signals cannot be definitively assigned; those corresponding to I, D or E and E or D are assigned by comparison of their chemical shifts to those of comparable carbonyls in isomer **3a** (we could not resolve the expected satellite coupling to ^{183}W of these low-intensity signals). The signal at 228.0 ppm is assigned to the Ir−Ir bridging carbonyl F, and the resonance at 177.6 ppm is assigned to the iridium-coordinated radial carbonyl H, the latter showing cis and trans P−C coupling to the axial- and radial-ligated phosphines, respectively. Carbonyl G is assigned on the basis of its cis P−C coupling to the radial phosphine ligand. A close inspection of the COSY spectrum suggests the assignment of the resonance at 161.5 ppm as A; this signal shows long-range trans coupling to G (Figure 8). Carbonyls B and C are trans to PPh_3 (through Ir) and Cp (through W), respectively, and we are not able to conclusively distinguish between these resonances at present.

Ligand fluxionality commences upon warming **3** above 191 K. The contour plot for **3** at 211 K (Figure 9) reveals site exchanges for the major isomer (**3a**) only (the minor isomer **3b** is not sufficiently abundant to afford cross-peaks, restricting the utility of the EXSY data to postulating exchange pathways for the more abundant isomer). Exchanges corresponding to a, a′ ↔ f and c, c′ ↔ d are observed, which we propose are due to two separate processes (note, however, that we were not able to discriminate energetically between these processes by lowering the temperature at which the EXSY spectrum was attained; the exchange pathways are therefore proposed very cautiously). The exchange a, a′ ↔ f is consistent with ligand mobility about the Ir_3 face with a carbonyl distribution in the intermediate reminiscent of the D_{2d} intermediate implicated in the $M_4(CO)_{12}$ exchange pathway[8] (Scheme 6). The exchange of carbonyls c, c′ and d probably involves scrambling about a WIr_2 face (Scheme 7) for which the direct pathway (two

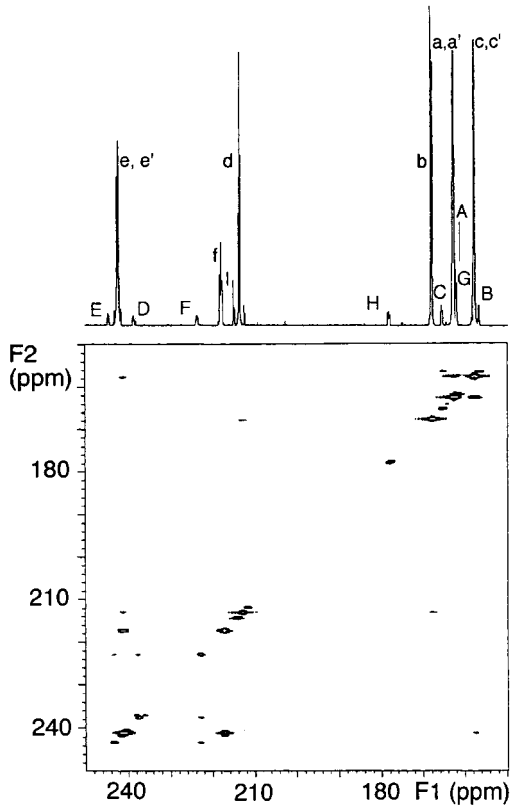

Figure 8. ^{13}C NMR COSY spectrum of $CpWIr_3(\mu\text{-}CO)_3(CO)_6(PPh_3)_2$ (**3**) in CD_2Cl_2 at 191 K.

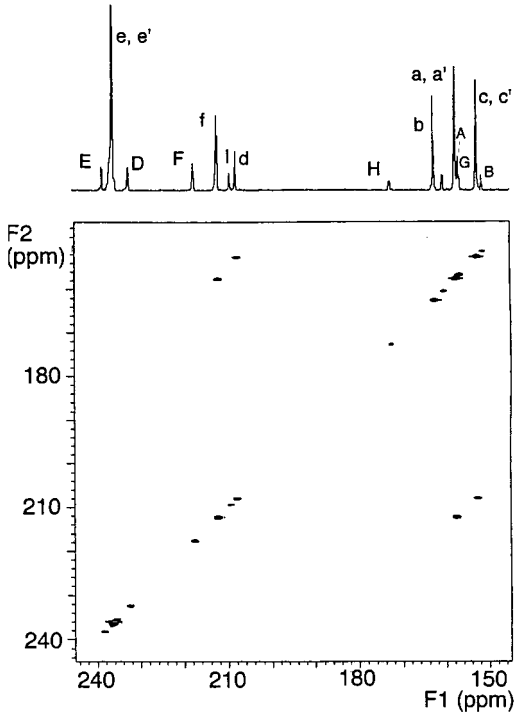

Figure 9. ^{13}C NMR EXSY spectrum of $CpWIr_3(\mu\text{-}CO)_3(CO)_6(PPh_3)_2$ (**3**) in CD_2Cl_2 at 211 K.

steps) requires an intermediate with six bridging carbonyls; we therefore prefer the longer pathway, which proceeds through two all-terminal intermediates in which the phosphines and Cp ligand prevent a merry-go-round process.

NMR Studies of $CpWIr_3(\mu\text{-}CO)_3(CO)_7(PMe_3)$ (4). $CpWIr_3(\mu\text{-}CO)_3(CO)_7(PMe_3)$ (**4**) is fluxional on the NMR

Scheme 6: CO Mobility about the Ir_3 Face in 3a and 5a

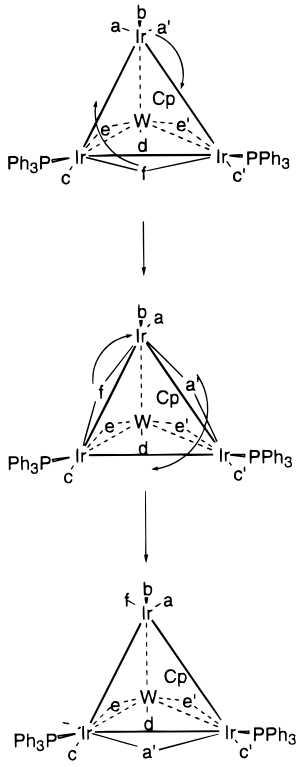

Scheme 7: CO Mobility about a WIr_2 Face in 3a and 5a

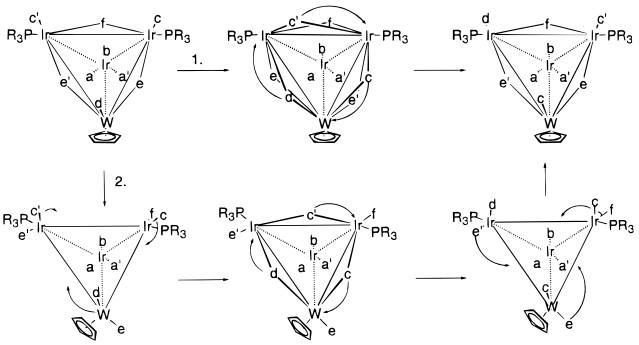

time scale, with one broad resonance observed above 298 K (^{13}C NMR, CD_2Cl_2/CS_2) or 273 K (^{31}P NMR, CD_2Cl_2). On cooling to 173 K in CD_2Cl_2, two signals are resolved in the ^{31}P NMR spectrum at −25.0 and −31.8 ppm (ratio 5:3, Figure 10). On cooling to 163 K, the ^{13}C NMR spectrum in CD_2Cl_2/CS_2 also decoalesces into signals corresponding to two isomers (Figure 11). The resonances in the ^{13}C NMR spectrum (Figure 11) corresponding to isomer **4a** exhibit a pattern similar to that of **2a**. At 163 K, resonances for isomer **4a** are observed at 209.5 (a, a′), 206.6 (b, b′), 202.2 (c), 177.7 (f), 174.9 (d, d′), and 158.0 (e, e′) ppm, with the relative intensities 2:2:1:1:2:2. The signal at 209.5 ppm shows coupling to ^{183}W (J_{WC} = 152 Hz) and is assigned to W-bound terminal carbonyls. The signals at 206.6 and 202.2 ppm are assigned to carbonyls bridging Ir−Ir vectors; isomer **4a** therefore possesses a triiridium basal plane. The signals at 177.7 and 174.9 ppm are assigned to three radial carbonyls, and the signal at 158.0 ppm is assigned to two axially coordinated carbonyls; isomer **4a** therefore has an apically coordinated cyclopentadienyl group and

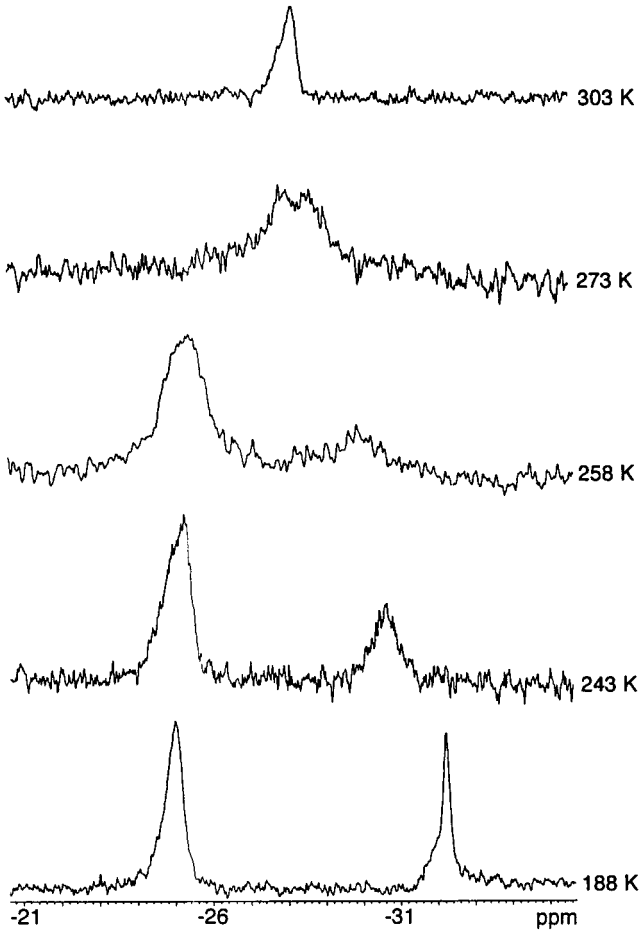

Figure 10. Variable-temperature ^{31}P NMR spectroscopic study of $CpWIr_3(\mu\text{-}CO)_3(CO)_7(PMe_3)$ (**4**) in CS_2/CD_2Cl_2.

axially coordinated phosphine, with the molecular symmetry evident from the ^{13}C NMR spectrum confirming that these ligands are trans-disposed via a W−Ir vector and that **4a** has the same configuration as **2a** (Figure 3). The configuration of **4a** corresponds to that observed in our earlier X-ray structural study.[37] As with **2**, the COSY experiment of **4** (Figure 12) reveals coupling between the Ir−Ir bridging carbonyls b, b′ and c. The signals in the ^{13}C NMR spectrum corresponding to the major isomer **4b** are fully analogous to those of the structurally characterized **2b**. As with isomer **2b**, the ^{13}C NMR spectrum of **4b** is as yet incompletely assigned (we are not able to discriminate between axial and apical carbonyl resonances). At 163 K, resonances for configuration **4b** are observed at 240.6 (E), 232.2 (D), 211.6 (F), 210.8 (J), and 179.4 (H) ppm. The COSY spectrum (Figure 12) reveals coupling between the W−Ir bridging carbonyls E and the Ir−Ir bridging carbonyl F, presumably due to asymmetric bridging of the W−Ir carbonyls. A small cross-peak between the signals at 158.4 and 160.8 ppm in the COSY spectrum leads us to tentatively assign these signals as arising from coupling between an axially ligating carbonyl (G or I) and an apical carbonyl (A or B); both pairs of carbonyls are situated in a transoid arrangement. The remaining specific assignments follow those for configuration **2b**, above; as with **2b**, it is not possible to assign the ligation site of the basal cyclopentadienyl ligand.

An EXSY spectrum of **4** at 178 K (Figure 13) reveals site exchanges corresponding to a, a′ ↔ b, b′; a, a′ ↔ d, d′; a, a′ ↔ e, e′; b, b′ ↔ d, d′; b, b′ ↔ e, e′; b, b′ ↔ f; d, d′ ↔ e, e′; and c ↔ d, d′ for isomer **4a**, the same as those observed previously with **2a**; the carbonyls of **4a** are therefore proposed to exchange via a concerted merry-go-round process as shown in Scheme 5.

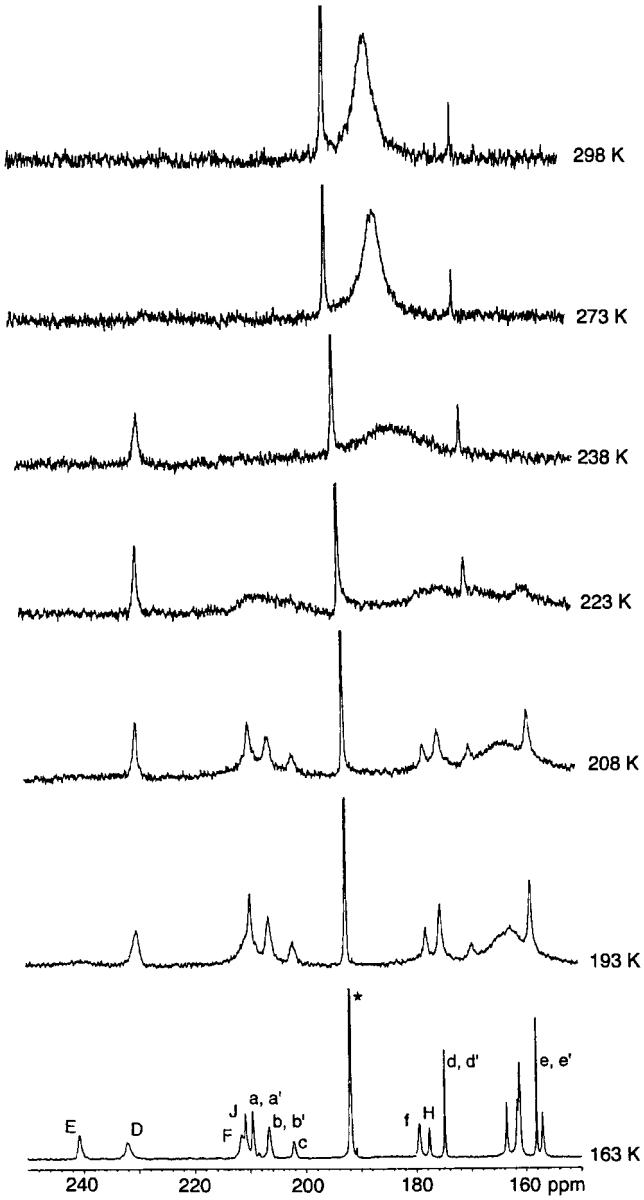

Figure 11. Variable-temperature ^{13}C NMR spectroscopic study of $CpWIr_3(\mu\text{-}CO)_3(CO)_7(PMe_3)$ (**4**) in CS_2/CD_2Cl_2 (★ ≡ CS_2).

NMR Studies of $CpWIr_3(\mu\text{-}CO)_3(CO)_6(PMe_3)_2$ (5). The room-temperature ^{13}C and ^{31}P NMR spectra of **5** in CD_2Cl_2 are above coalescence, but all exchange processes are very slow at 193 K (Figures 14 and 15). At this temperature, the ^{31}P NMR spectrum shows three resonances (ratio 20:1:1) corresponding to two isomers. Similarly, the ^{13}C NMR spectrum at 193 K displays signals corresponding to two isomers. A comparison of the ^{13}C and ^{31}P NMR spectra of **5** at this temperature with those of **3** at 191 K (Figure 6) leads us to suggest that isomers **5a** and **5b** have the same triradial and radial, diaxial (or diradial, axial) geometries as **3a** and **3b**, respectively. At 193 K, resonances in the ^{13}C NMR spectrum are observed for **5a** at 247.4 (e, e′), 225.9 (f), 214.8 (d), 167.5 (b), 164.0 (a, a′), and 162.2 (c, c′) ppm,

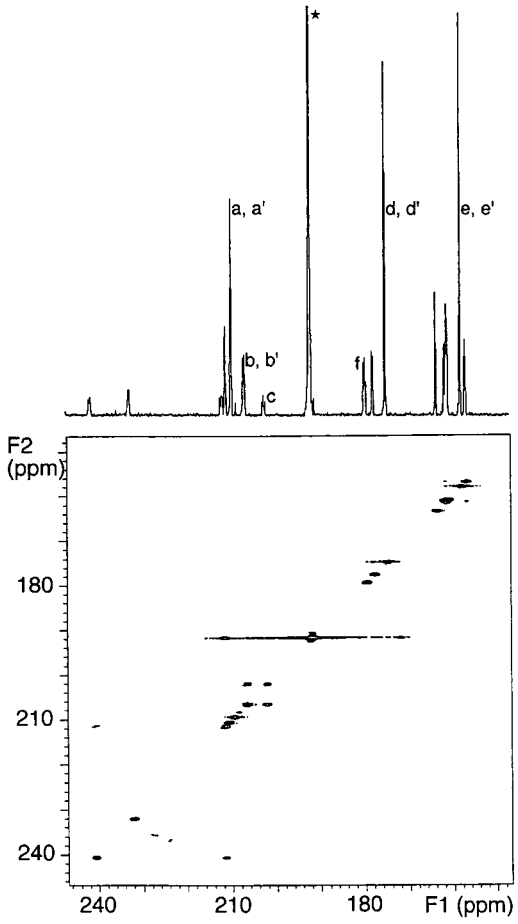

Figure 12. ^{13}C NMR COSY spectrum of $CpWIr_3(\mu\text{-}CO)_3(CO)_7(PMe_3)$ (**4**) in CS_2/CD_2Cl_2 at 163 K (★ ≡ CS_2).

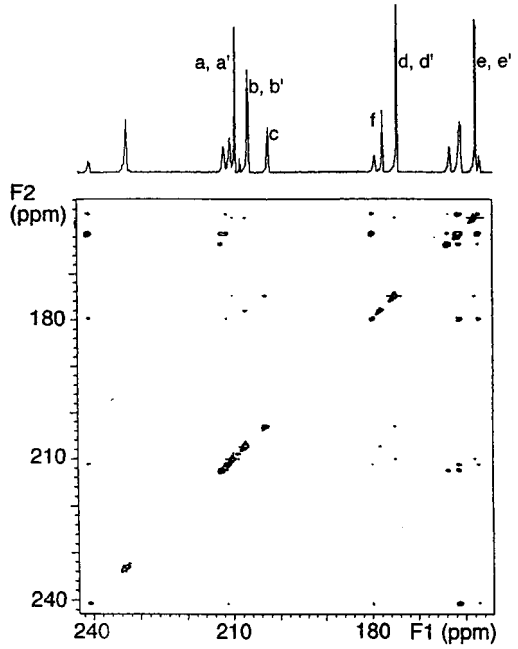

Figure 13. ^{13}C NMR EXSY spectrum of $CpWIr_3(\mu\text{-}CO)_3(CO)_7(PMe_3)$ (**4**) in CD_2Cl_2 at 178 K.

with the relative intensities 2:1:1:1:2:2. A COSY experiment was used to establish the position of the cyclopentadienyl ligand in **5a** (Figure 16). The presence of a long-range trans coupling between b and d demonstrates the radial coordination of the cyclopentadienyl

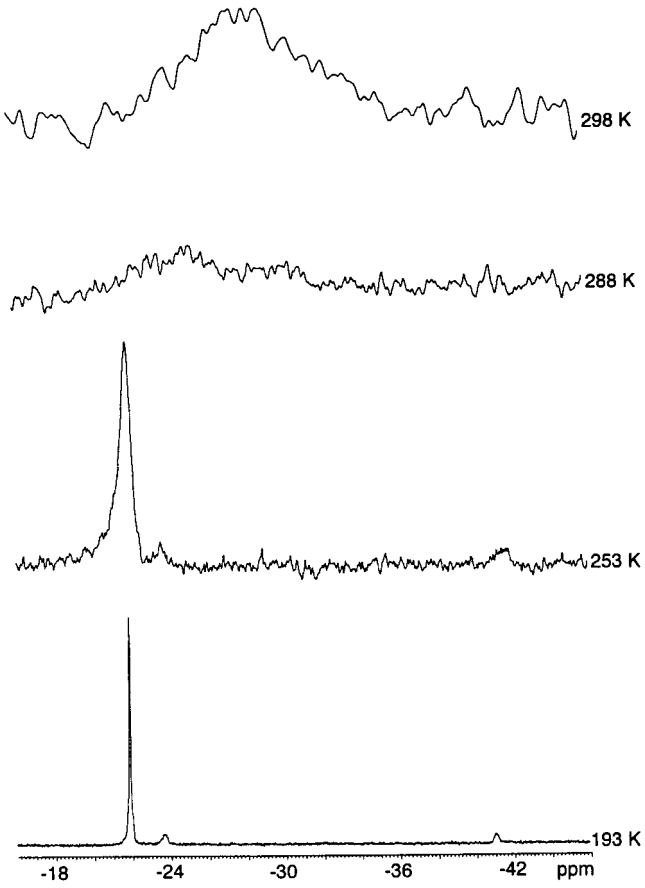

Figure 14. Variable-temperature ^{31}P NMR spectroscopic study of $CpWIr_3(\mu\text{-}CO)_3(CO)_6(PMe_3)_2$ (**5**) in CD_2Cl_2.

ligand; **5a** is thus, like **3a**, an example of a cluster with a heretofore unobserved triradial coordination geometry. Resonances for the minor isomer **5b** are observed in the ^{13}C NMR spectrum at 249.0 (D or E), 244.7 (E or D), 225.8 (F), 216.1 (I), 180.8 (H), 166.7 (C or B), 163.5 (G), 165.9 (A), and 159.2 (B or C) ppm, all with intensity 1, the specific assignments of which follow those outlined above for **3b**. The coincident nature of carbonyls f and F is unusual and differs from the pattern identified for carbonyls f and F in **3**. The COSY spectrum of **5**, however, reveals the presence of a small cross-peak between the signal at 225.9 ppm (f and F) and 244.9 ppm (E or D), as well as a clear cross-peak between the signals at 225.9 ppm (f and F) and 247.4 ppm (e, e′). The COSY spectrum of **3** reveals similar cross-peaks.

An EXSY spectrum of **5** (Figure 17) reveals site exchanges corresponding to a, a′ ↔ f and c, c′ ↔ d for **5a**, the same as was observed earlier with the analogous isomer **3a**. The proposed exchanges follow those outlined for **3a**, the mechanisms being shown in Schemes 2 and 3. As with **3b**, isomer **5b** was present in insufficient amounts to allow exchange processes to be observed and identified.

Discussion. Heterometal incorporation into a well-studied homometallic cluster is of fundamental importance, and the present study has afforded the possibility of examining its influence upon such properties as reaction kinetics, product distribution, and ligand fluxionality. Our earlier report showed vastly increased reaction rates for ligand substitution upon introduction of the mid-transition metal.[37] The present studies

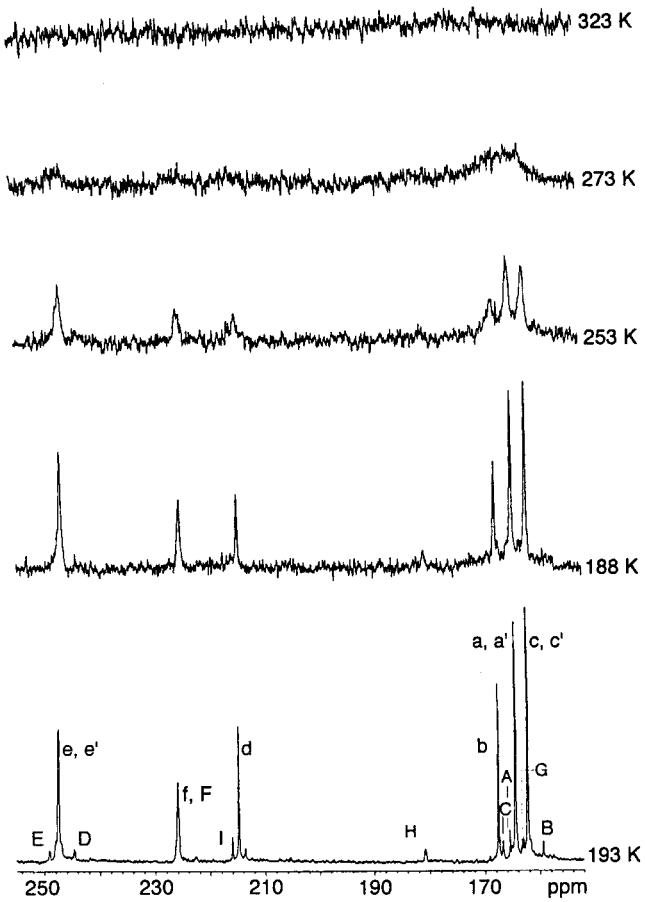

Figure 15. Variable-temperature ^{13}C NMR spectroscopic study of $CpWIr_3(\mu\text{-}CO)_3(CO)_6(PMe_3)_2$ (**5**) in CD_2Cl_2.

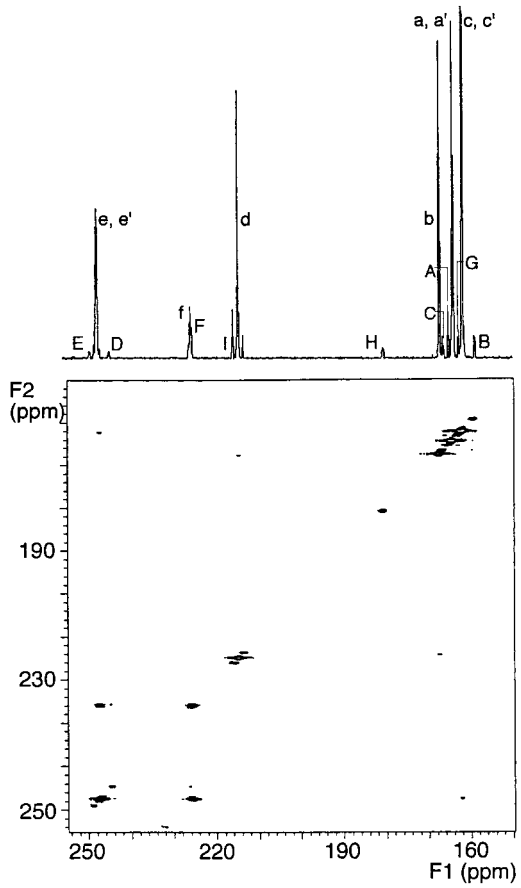

Figure 16. ^{13}C NMR COSY spectrum of $CpWIr_3(\mu\text{-}CO)_3(CO)_6(PMe_3)_2$ (**5**) in CD_2Cl_2 at 193 K.

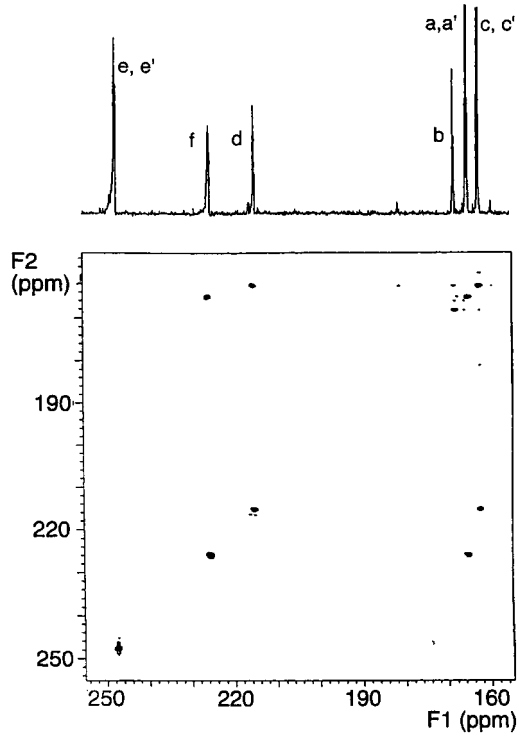

Figure 17. ^{13}C NMR EXSY spectrum of $CpWIr_3(\mu\text{-}CO)_3(CO)_6(PMe_3)_2$ (**5**) in CD_2Cl_2 at 228 K.

permit a comparison of isomer distribution and carbonyl scrambling pathways. Roulet et al. have shown that, on progressing from ligand-substituted tetrairidium clusters to ligand-substituted rhodium−triiridum clusters, the positional NMR sequence bridging > radial > axial ≈ apical observed for Ir-ligated carbonyls is maintained.[33,34] Conceptual replacement of two iridium atoms in $Ir_4(CO)_{12}$ affords $Rh_2Ir_2(CO)_{12}$; ligand-substituted analogues of the latter reveal the same trend in the NMR chemical shifts.[36] Our work has involved the conceptual replacement of an $Ir(CO)_3$ vertex in $Ir_4(CO)_{12}$ by a $CpW(CO)_2$ vertex affording $CpWIr_3(CO)_{11}$, and we have shown that ligand-substituted derivatives of the tungsten−triiridium cluster follow the same trends in NMR chemical shift of carbonyl ligands as do those of the "parent" tetrairidium cluster.[1,41] The current studies have conclusively established some of the configurations of $CpWIr_3(\mu\text{-}CO)_3(CO)_{8-n}(L)_n$ (L = PPh_3, PMe_3; n = 1, 2), permitting comment on the effect of ligand and metal variation upon product distribution. Replacement of PPh_3 by the more basic and sterically less demanding PMe_3 has essentially no impact on isomer structure or ratio for $CpWIr_3(\mu\text{-}CO)_3(CO)_6(L)_2$. For the monophosphine derivatives, PPh_3 affords significant amounts of three isomers with the axial PPh_3, apical Cp form the most abundant, while PMe_3 affords two isomers with the radial PMe_3-containing isomer present in greater amounts; PPh_3 uniquely affords a third isomer with an axial PPh_3, a result that can perhaps be rationalized on steric grounds as the cone angles decrease in the order PPh_3 (145°) > Cp (136°) > PMe_3 (118°). The

(41) Waterman, S. M.; Humphrey, M. G.; Hockless, D. C. R. *J. Organomet. Chem.* **1998**, *555*, 25.

coordination geometries of the $CpWIr_3(\mu\text{-}CO)_3(CO)_{8-n}(L)_n$ can be contrasted with those of $Ir_4(\mu\text{-}CO)_3(CO)_{8-n}(PR_3)_{n+1}$. For $n = 1$, examples of radial, axial coordination in the iridium system are extant, but the axial, apical mode of **2a** and **4a** is unprecedented with tetrairidium clusters. For $n = 2$, the radial, diaxial mode in the structurally characterized isomer of **3** is only observed in the iridium system with polydentate ligands (for monodentate ligands, diradial, axial coordination geometry is preferred); the triradial geometry of **3a** and **5a** is unprecedented with tetrairidium clusters. There are clearly dramatic differences in isomer preference for monodentate ligand derivatives in the Ir_4 and WIr_3 series of clusters.

These differences in isomer distribution between the Ir_4 and WIr_3 systems render comparisons of CO mobility difficult. The structural study of **4a** reveals a symmetric bridging carbonyl distribution. $Ir_4(\mu\text{-}CO)_3(CO)_7(L)_2$ examples with this carbonyl geometry exchange CO ligands by a merry-go-round process at all faces, which proceed by way of an unbridged intermediate (Scheme 3), a process we suggest is observed with the structurally similar **2a** and **4a**. The novel geometries observed with **3a** and **5a** obviously preclude comparisons with related derivatives in the tetrairidium system, but the pathway postulated in Scheme 6 for carbonyl fluxionality in mixed metal clusters provides an interesting analogue of the D_{2d}-symmetry intermediate implicated in $Ir_4(CO)_{12}$ fluxionality.

Acknowledgment. We thank the Australian Research Council for support of this work and Johnson-Matthey Technology Centre for the generous loan of $IrCl_3$. M.G.H. held an ARC Australian Research Fellowship and holds an ARC Senior Research Fellowship. Professor B. E. Mann (Sheffield) is thanked for helpful discussions.

Supporting Information Available: A summary of ^{13}CO chemical shifts observed with P-donor ligand-substituted derivatives of **1.** This material is available free of charge via the Internet at http://pubs.acs.org.

OM9902885